The *Swift* short gamma-ray burst rate density: implications for binary neutron star merger rates

D. M. Coward,[1]*† E. J. Howell,[1] T. Piran,[2] G. Stratta,[3] M. Branchesi,[4,5] O. Bromberg,[2] B. Gendre,[3,6] R. R. Burman[1] and D. Guetta[6,7]

[1]*School of Physics, University of Western Australia, Crawley WA 6009, Australia*
[2]*Racah Institute of Physics, The Hebrew University, Jerusalem 91904, Israel*
[3]*ASI Science Data Center, via Galileo Galilei, 00044 Frascati (RM), Italy*
[4]*DiSBeF – Università degli Studi di Urbino 'Carlo Bo', I-61029 Urbino, Italy*
[5]*INFN, Sezione di Firenze, I-50019 Sesto Fiorentino, Italy*
[6] *INAF – Osservatorio Astronomico di Roma, Via Frascati 33, I-00040 Monteporzio Catone, Roma, Italy*
[7]*Department of Physics and Optical Engineering, ORT Braude, PO Box 78, Karmiel, Israel*

ABSTRACT

Short gamma-ray bursts (SGRBs) observed by *Swift* potentially reveal the first insight into cataclysmic compact object mergers. To ultimately acquire a fundamental understanding of these events requires pan-spectral observations and knowledge of their spatial distribution to differentiate between proposed progenitor populations. Up to 2012 April, there are only some 30 per cent of SGRBs with reasonably firm redshifts, and this sample is highly biased by the limited sensitivity of *Swift* to detect SGRBs. We account for the dominant biases to calculate a realistic SGRB rate density out to $z \approx 0.5$ using the *Swift* sample of peak fluxes, redshifts and those SGRBs with a beaming angle constraint from X-ray/optical observations. We find an SGRB lower rate density of 8^{+5}_{-3} Gpc^{-3} yr^{-1} (assuming isotropic emission) and a beaming corrected upper limit of 1100^{+700}_{-470} Gpc^{-3} yr^{-1}. Assuming a significant fraction of binary neutron star mergers produce SGRBs, we calculate lower and upper detection rate limits of $(1–180)$ yr^{-1} by an Advanced LIGO (aLIGO) and Virgo coincidence search. Our detection rate is similar to the lower and realistic rates inferred from extrapolations using Galactic pulsar observations and population synthesis.

Key words: gravitational waves – techniques: miscellaneous – gamma-ray burst: individual – stars: neutron.

1 INTRODUCTION

It is generally accepted that 'long' ($T_{90} > 2$ s)[1] gamma-ray bursts (GRBs) are linked to the core collapse of massive stars (collapsars) (Woosley 1993; Paczynski 1998; MacFadyen & Woosley 1999). For several cases, the GRBs are firmly associated with Type Ib/c supernovae (e.g. Hjorth et al. 2003; Stanek et al. 2003). This strongly suggests that they are linked to the end point of massive stellar evolution. In contrast, 'short' ($T_{90} < 2$ s) gamma-ray bursts (SGRBs) have a less certain origin.

The first breakthrough to understanding the nature of SGRBs was made in 2005 after the launch of the NASA *Swift* satellite

(Gehrels et al. 2004). Prompt localizations and deep afterglow searches yielded the first redshifts and investigations of their progenitor environments. By late 2011, about three dozen SGRBs had been localized by *Swift*. Among them, about 50 per cent have optical detections and about one-third have redshift determinations based on host-galaxy spectroscopy.

Binary neutron star mergers (NS-NS) or neutron star–black hole (NS-BH) mergers are favoured as the progenitors for SGRBs, based on the association of some SGRBs with an older stellar population, as compared to long GRBs. Evidence for the origin of SGRBs in the final merger stage comes from the host-galaxy types (e.g. Lee, Ramirez-Ruiz & Granot 2005; Zheng & Ramirez-Ruiz 2007). Kicks imparted to NSs at birth will produce velocities of several hundred km s^{-1}, implying that binary inspiraling systems may occur far from their site of origin. Fong, Berger & Fox (2010) using *Hubble Space Telescope* observations to measure SGRB-galaxy offsets find that the offset distribution compares favourably with the predicted distribution for NS-NS binaries.

★E-mail: david.coward@uwa.edu.au
†Australian Research Council Future Fellow.
[1] T_{90} is the duration in which the cumulative counts are from 5 to 95 per cent above background.

Despite this progress, unambiguous identification of burst types continues to be a problem. The various ambiguities have motivated several authors to redefine different classes of GRBs via a number of properties including spectral features, associated supernova, stellar population, host galaxy, location in the host galaxy and progenitor type (Zhang et al. 2007). Some authors also suggest a third intermediate population of bursts based on the existing T_{90} scheme (Horváth et al. 2008) with a lower than average peak-flux distribution (Veres et al. 2010).

Furthermore, work by Bromberg et al. (2012a) shows that categorizing bursts as SGRBs based on T_{90} is satellite dependent. They find that $2\,s > T_{90}$ is statistically reasonable for Burst and Transient Source Experiment (BATSE) bursts, but not accurate for *Swift* bursts. To quantify this uncertainty, for a 0.7-s burst they show that there is an equal probability of its being either long or short. We account for this uncertainty, and its effect on the intrinsic SGRB rate; we scale our SGRB rate estimates using a refinement of these probabilities that incorporates a power law fit to the bursts within the *Swift* energy band.

Around 20 per cent of the SGRBs detected by *Swift* have been followed by an extended emission lasting up to 100 s (hereafter SGRB-EE) (Norris & Bonnell 2006; Perley et al. 2008) leading to suggestions that different progenitor types produce these bursts (Norris, Gehrels & Scargle 2011). Troja et al. (2008) argue that SGRB-EE could be NS-BH mergers based on their galaxy off-sets. Other candidate systems include the birth of a rapidly rotating proto-magnetar produced via NS-NS merger or accretion-induced collapse of a white dwarf (Metzger, Quataert & Thompson 2008; Bucciantini et al. 2012). In the following, we have considered separately the normal SGRBs and the SGRB-EE to take this uncertainty in the progenitor nature into account.

SGRB observations could potentially play a more important role in constraining compact object merger rates on two fronts as more data become available. First, as a direct consistency check of the binary merger rates inferred from binary pulsars and population synthesis. Secondly, as a constraint on the progenitor scenario and the engine that drives the emissions. Both are critical issues for solving the puzzle of the origin of SGRBs and their links to compact object mergers.

There are two popular but different methods employed for estimating NS-NS merger rates. The first uses extrapolation from the observed sample of NS binaries inferred from pulsar observations (Narayan, Piran & Shemi 1991; Kalogera et al. 2006); the second uses population synthesis simulations (Belczynski et al. 2007), where several unknown model parameters are constrained by observations and others are assumed from theory. Abadie et al. (2010) (hereafter Ab10) assessed the rates from these techniques, defining lower and realistic rate densities of 10 and 1000 $Gpc^{-3}\,yr^{-1}$, respectively. These rates are uncertain by one to two orders of magnitude because of the small number of observed Galactic binary pulsars, and from poor constraints in population-synthesis models.

Within 5 yr, coordinated gamma-ray, X-ray, optical and gravitational-wave observations may allow the strong gravity regime of the central engine of compact object mergers to be probed. Such 'multi-messenger' observations provide the opportunity to probe these events across a vast energy spectrum and to constrain the progenitor populations of SGRBs. Furthermore, co-ordinated optical and gravitational-wave searches may play an important role in confirming the first direct gravitational-wave observations of compact object mergers (Coward et al. 2011). It is becoming increasingly important to constrain the rate of compact object mergers

and their proposed optical counterparts in the context of upcoming gravitational-wave searches.

The scarcity of SGRB observations and the poorly understood biases in the current data have made it challenging to calculate the SGRB rate density with meaningful uncertainties. Previous work using GRB flux-limited samples either assumes or derives models for the SGRB luminosity function and rate evolution of the sources, e.g. Guetta & Piran (2006) find an SGRB rate density of $8-30\,Gpc^{-3}\,yr^{-1}$, assuming isotropic emission. Another study (Dietz 2011) calculates a higher NS-NS merger rate of about $7800\,Gpc^{-3}\,yr^{-1}$, but assuming the emissions are beamed with small opening angles.

In this paper, we calculate a beaming-corrected SGRB rate density using the *Swift* sample of SGRB peak fluxes, redshifts and inferred beaming angles from X-ray observations. For our GRB selection criteria, we use the Jochen Greiner catalogue of localized GRBs (see Table 1) and select bursts indicated as short that have reliable redshifts up to 2012 April. From this selection of nine bursts, we omit the burst GRB 090426, which is possibly linked to the death of a massive star based on its galaxy off-set and optical and X-ray emissions. We also note that although GRB 100816A has shown certain characteristics not consistent with an SGRB classification, it cannot be clearly ruled out; additionally, its redshift of $z = 0.8$ will not influence our results significantly.

Table 1. SGRB peak fluxes, T_{90} and redshifts taken from the *Swift* online catalogue and http://www.mpe.mpg.de/~jcg/grbgen.html used to calculate Poisson rates. We use the 20-ms peak photon fluxes from the BAT2 catalogue where possible – those marked by * are 1-s peak photon fluxes. †We set a lower limit on the jet opening angle from the time when the *Swift* XRT monitoring stopped.

SGRB	T_{90} (s)	θ_j (deg)	z	Peak flux (ph s^{-1} cm^{-2})	Ref.
101219A*	0.6	–	0.718	4.1	(1)
100117A*	0.3	–	0.92	2.9	(2)
090510A*	0.3	–	0.903	9.7	(3)
080905A^a	1.0	–	0.122	6.0	(4)
070724A	0.4	>11†	0.457	2.0	(5)
061217A	0.2	–	0.827	2.4	(6)
051221A*	1.4	7^b	0.547	12.0	(7)
050509B	0.73	–	0.225	3.7	(8)
SGRB-EE					
071227A	1.8	>16†	0.383	4.4	(9)
070714B	64	>6†	0.923	10.0	(10)
061210	85	>12†	0.409	62.9	(11)
061006	129	>6†	0.437	15.8	(12)
060614	109	12^c	0.125	25.0	(13)
050724	96	>25†	0.258	12.8	(14),(15)

^{a} The proposed host galaxy at $z = 0.1218$ for GRB 080905A (Rowlinson et al. 2010) is a strong outlier to the Yonetoku relation (Yonetoku et al. 2004). A redshift $z > 0.8$ would make it consistent (Gruber et al. 2012).
^{b} The detection of a jet break was observed for GRB 051221A in X-rays (Soderberg et al. 2006) at about 5 d post-burst, or $\theta \sim 7°$.
^{c} Jet break identified at 1.4 d post-burst, circumburst density $n = 10\,cm^{-3}$ and $E_{iso} = 2.5 \times 10^{51}$ ergs. References – (1) GCN 11518, (2) Fong et al. (2011), (3) Ackermann et al. (2010), (4) Rowlinson et al. (2010), (5) Berger et al. (2009), (6) Berger et al. (2007), (7) Soderberg et al. (2006), (8) Gehrels et al. (2005). The SGRBs below the line are classified as SGRB-EE – (9) Caito et al. (2010), (10) Graham et al. (2009), (11) Berger et al. (2007), (12) Berger et al. (2007), (13) Della Valle (2006), (14) Berger et al. (2005), (15) Gruppe et al. (2006).

We avoid using an SGRB luminosity function, models for progenitor rate evolution and a beaming angle distribution, all of which have large uncertainties. Instead, we focus on observed and measured parameters that take into account selection effects that modify *Swift*'s detection sensitivity to SGRBs. Finally, we use our SGRB rate density estimates to infer a detection rate of binary NS mergers by Advanced LIGO (aLIGO) and Virgo interferometers. Despite the poor statistics, this approach gives meaningful results and can be followed up when a larger sample of SGRB observations becomes available.

2 SGRB BEAMING CONSTRAINTS

The currently favoured emission model for SGRBs is a compact object merger triggering an explosion causing a burst of collimated γ-rays (Eichler et al. 1989; Narayan, Paczynski & Piran 1992; Lee, Ramirez-Ruiz & Granot 2005) powered by accretion on to the newly formed compact object. The ultra-relativistic outflow is eventually decelerated by interaction with the interstellar medium to produce a fading X-ray and optical afterglow. After the jet Lorentz factor Γ decreases to $\Gamma \sim \theta_j^{-1}$, where θ_j is the jet opening half-angle, the afterglow becomes observable from viewing angles greater than θ_j.

Only two SGRBs have identifiable jet breaks (see Coward et al. 2011, and references therein): GRB 050709 ($\theta_j \sim 14°$ – detected by the *HETE* satellite) and GRB 051221 ($\theta_j \sim 7°$). These beaming angles are not necessarily agreed upon, mainly because the afterglow jet-break times obtained from X-ray or optical light curves are notoriously difficult to identify at late times, and the emissions are generally fainter in X-rays and optical compared to those of long bursts. Furthermore, the inferred beaming angles are model dependent (Sari, Piran & Halpern 1999) and sensitive to the circumburst environment.

For the following rate density calculations, we employ the standard fireball model (e.g. Sari et al. 1999) to estimate the jet opening half-angle using the minimum jet-break times from X-ray observations:

$$\theta_j = 0.161[t_j/(1+z)]^{3/8}(n\eta/E_{iso})^{1/8} \text{ rad,} \quad (1)$$

where t_j, the jet-break time, is the time in days when the light-curve decay index changes from -1 to -2. The parameter n is the circumburst density in cm^{-3}, η is the fraction of GRB energy observed in the prompt emission and E_{iso} is the prompt isotropic equivalent energy in 10^{52} erg. We assume an average of $n = 1\,cm^{-3}$ and $\eta = 0.1$ for our SGRB sample.

The circumburst density for both long- and short-duration GRBs is quite scattered, and typically ranges from 0.001 to $10\,cm^{-3}$. Kopac et al. (2012) showed that n for SGRBs is similar to the one derived for long bursts (Gendre, Corsi & Piro 2006), implying that the local density should be similar for both collapsars and mergers. Contrary to this, Fong et al. (2012) argue that SGRBs are located in typically smaller circumburst densities, supported by their constraint of $n = 0.01–0.1\,cm^{-3}$ for GRB 111020A. For definiteness, we use $0.01\,cm^{-3}$ to calculate lower limits on the beaming angle for SGRBs without a measured jet break. Alternatively, for the SGRB-EE sample we use $n = 1\,cm^{-3}$, because the only confirmed SGRB-EE with a jet break, GRB 060614, is constrained to $n = 10\,cm^{-3}$ (Della Valle 2006).

The difficulty of measuring jet breaks leads to a bias in obtaining jet angles favouring those bursts that have very bright X-ray/optical afterglows and/or relatively short jet-break times. Hence, the true average of the SGRB jet angle distribution will be greater than that based on the very small sample used in this work. Nonetheless,

given the lack of knowledge of the SGRB angle distribution, both theoretically and observationally, we choose to employ the small number of inferred SGRB beaming angles and lower limits from X-ray/optical observations.

To extend the very small measured beaming angle sample, we constrain the minimum beaming angles for those SGRBs that have X-ray afterglow light curves available up to at least 1 d from the trigger. The following five SGRBs: GRB 100816A, GRB 071227A, GRB 070714B, GRB 061006 and GRB 050724 satisfy this criterion. We set a lower limit on the jet opening angle from the time when the *Swift* X-ray Telescope (XRT) monitoring stopped. We compute E_{iso}, from the literature, if available, or from the quoted fluences in the Gammaray Co-ordinates Network (GCN) circulars by estimating the corresponding E_{iso} in the $1–10^4$ keV rest-frame energy range. For the GRB energy spectrum, we use the broken power-law fit, termed the Band model (Band 2006), or cut-off power law with spectral parameters where known. If the spectral parameters are unknown, we simply rescale the fluence by $4\pi d_L^2/(1+z)$, where d_L is the luminosity distance.

3 EMPIRICAL SGRB RATE MODEL

A Poisson GRB rate can be estimated from small number statistics using V_{max} (Piran 1992; Cohen & Piran 1995), where V_{max} is the maximum volume within which an SGRB with observed peak flux, F_p, could be detected for a given satellite detector with detection sensitivity F_{Lim}. While V_{max} has been used previously (e.g. Guetta & Della Valle 2007) to estimate rates of low-luminosity GRBs (see also Coward 2005), we extend the rate estimate method to account for biases in the *Swift* GRB redshift and peak-flux sample.

First, the low energy detection bandwidth of *Swift* (15–150 keV) in comparison with BATSE's 50–300 keV results in a bias against SGRBs which typically have harder emissions. Secondly, the *Swift* detection threshold is not simply defined by the detector sensitivity, but by a complex triggering algorithm. Both these effects manifest as a bias against *Swift* detecting SGRBs, i.e. a smaller proportion of bursts has been detected by *Swift* (∼10 per cent). The latter effect results from the detection process employed by BAT, the *Swift* coded-aperture mask γ-ray detector. In addition to requiring an increased photon count rate above background (the sole triggering criterion used for BATSE), BAT employs a second stage in which an image is formed by accumulating counts for up to 26 s (Band 2006).

We attempt to crudely correct for these biases by using the observed SGRB rate from BATSE as a rate calibration for the *Swift* SGRB rate. Because BATSE operated at different energy thresholds and trigger sensitivities, for consistency we take all BATSE SGRBs with 64-ms peak flux when the trigger threshold was set to 5.5σ in the 50–300 keV energy range (total live operation time of 3.5 yr). This yields 32 SGRBs $sr^{-1}\,yr^{-1}$, assuming an effective BATSE field of view (FoV) of π sr (Band 2003). The ratio of the rate of BATSE to *Swift* SGRBs, $R_{B/S} = 6.7$, is used to calibrate the observed *Swift* SGRB rate to estimate an intrinsic SGRB rate.

Because SGRBs occur over a short duration, it is more difficult (compared to long bursts) to produce a significant signal above background. Hence, instead of using the theoretical BAT sensitivity of $F_{Lim} = 0.4$ ph $s^{-1}\,cm^{-2}$, we employ a flux limit of 1.5 ph $s^{-1}\,cm^{-2}$, using the smallest 20-ms peak flux from the SGRB data.

Another detector-dependent selection effect arises from the limited energy bandpass of *Swift*, i.e. 15–150 keV. What is measured by *Swift* is not the bolometric peak flux, but a detector response and source-spectrum-dependent peak flux. We define the bolometric

isotropic-equivalent luminosity correction factor (Imerito et al. 2009)

$$C_{det}(e_1, e_2) \equiv \frac{\int_{E_1}^{E_2} E N(E)\, dE}{\int_{e_1}^{e_2} E N(E)\, dE}, \qquad (2)$$

where $[E_1 = 1, E_2 = 10\,000]$ keV spans the bolometric gamma-ray spectrum, and $[e_1, e_2]$ is the sensitivity band of *Swift*, i.e. 15–150 keV. For the source energy spectrum, $N(E)$, we employ the Band function (Band 2006), with spectral indices $\alpha = -1$, $\beta = -2.3$ and a rest-frame power-law break energy of 511 keV.

In addition, for high redshift sources, a higher energy component of the source spectrum is redshifted into the sensitivity band of the detector. The following factor, $k(z)$, accounts for the downshift of γ-ray energy from the burst to the observer's reference frame:

$$k(z) \equiv \frac{\int_{e_1}^{e_2} E N(E)\, dE}{\int_{(1+z)e_1}^{(1+z)e_2} E N(E)\, dE}. \qquad (3)$$

Taking into account the sensitivity reduction and k-correction, the SGRB all-sky rate can be inferred from the flux-limited SGRB sample in Table 1. We calculate the maximum distance d_{max}, with corresponding redshift z_{max}, that a burst at luminosity distance d_L could be detected given *Swift's* sensitivity F_{Lim}:

$$d_{max} = \sqrt{\frac{F_p k(z)}{F_{Lim} k(z_{Lim})}} d_L(z), \qquad (4)$$

where F_p is the observed peak flux and $k(z_{Lim})$ is the k-correction for a burst at the maximum limiting distance of detection for the sample. Given the large uncertainty in the SGRB luminosity function, we use the largest redshift from our sample, $z_{Lim} = 0.92$. We note that the bolometric correction, $C_{det}(e_1, e_2)$, cancels out in the above equation, because it is independent of redshift.

The corresponding maximum SGRB detection volume for each burst is defined as

$$V_{max} = \int_0^{z_{max}} \frac{dV}{dz}\, dz, \qquad (5)$$

where the volume element factor, dV/dz, and luminosity distance, $d_L(z)$, are calculated using a flat-Λ cosmology with $H_0 = 71$ km s^{-1} Mpc^{-1}, $\Omega_M = 0.3$ and $\Omega_\Lambda = 0.7$. This estimate (equation 5) is valid as long as the rate of SGRBs does not change significantly over the range $(0, z_{max})$. Since the detection range of SGRBs is quite small and typically $z < 1$, this approximation is valid.

To calculate the intrinsic rate of SGRBs requires accounting for the beaming angle, θ_j, of the jetted burst. Equation (6) expresses the beaming factor used to correct for the unobserved SGRBs that are not detected because the jet is misaligned with the detector:

$$B(\theta_j) = [1 - \cos(\theta_j)]^{-1}. \qquad (6)$$

To account for the fact that only a fraction of observed SGRBs have measured redshifts, we scale the rate density by the ratio of *Swift* bursts with redshift to those without redshifts, F_r. We use $F_r \approx 8/39$ and $6/12$ for SGRB and SGRB-EE, respectively. The time span encompassing all observations, $T \sim 6$ yr, is defined by the start of *Swift* observations to the time of the most recent SGRB in the sample and we account for the fractional sky coverage of *Swift*, $\Omega \approx 0.17$. To account for *Swift*'s reduced sensitivity for detecting SGRBs relative to BATSE, we use the ratio of the BATSE to *Swift* SGRB detection rate, which we approximate as $R_{B/S} = 6.7$. This converts the *Swift* SGRB rate into an intrinsic SGRB rate. We point out that this correction applies only to SGRB, and not SGRB-EE, because *Swift* is more sensitive to these longer emission bursts.

Finally, we calculate the probability of a GRB to be a non-collapsar, $P_{i(T_{90};\, P_L)}$ (Bromberg et al. 2012a), based on its T_{90} and a power-law fit to the gamma-ray spectrum in the 15−150 keV band. The study was refined (Bromberg et al. 2012b, in preparation) to show that a GRB with a hard power-law photon index ($P_L < 1.15$) has a larger chance of being a non-collapsar than a GRB with a soft photon index at the same T_{90}. We note that these probabilities do not influence the magnitude of the calculated rate densities significantly in this work.

Combining all detection parameters yields the Poisson SGRB rate density of a single (*i*th) burst and the total rate density for n bursts:

$$R_{SGRB} = \sum_i^n \frac{1}{V_{i(max)}} \frac{1}{F_r} \frac{1}{T} \frac{1}{\Omega} R_{B/S} B_i(\theta_j) P_{i(T_{90}; P_L)}. \qquad (7)$$

SGRBs may track the star formation rate (SFR) history, albeit with a time delay. The z_{max} that we derive for the most significant contributions to the rate density range $z = 0.2-0.4$. To investigate the effect of including SFR evolution, we recalculated a local rate density using an integrated differential rate equation using several different SFR models and volumes bounded by z_{max}. We find differences of a factor of about 2 between the local rate densities calculated using equation (7) and an integrated differential rate model. Also there are discrepancies at small z using different SFR models, highlighting that the models are not good fits at small z. Given that the uncertainties in the small z SFR are of the same scale as the change in the SFR from $z = 0$ to 0.3, e.g. see fig. 10 in Reddy & Steidel (2009), we do not include an evolution of the SGRB rate density in space.

We calculate lower rate estimates assuming no beaming. Upper rates are estimated using the observed beaming angle constraints for each burst, and if a beaming angle estimate is unavailable, we use the smallest inferred jet angle from the data, $\theta_j \sim 7°$. Given that the inferred average beaming angle of the jet is biased towards SGRBs with short jet-break times (see Section 2), our upper rate limit estimate is at the limit of plausibility.

We use the above SGRB rate density to infer a detection rate of binary NS mergers by advanced gravitational-wave interferometers. For aLIGO and Virgo interferometer sensitivities, the horizon distance D_h (all sky locations and orientation averaged over) for optimal detection of an NS-NS merger in a coincidence search is about 340 Mpc (cosmological redshift not included). For a direct comparison with Ab10, the detection rate is computed considering the noise power spectral density of a single interferometer, with $D_h = 197$ Mpc. Given the uncertainty in the beaming angle distribution, we define an optimal detection rate as a function of θ_j using the SGRB lower rate estimate, i.e. from $\theta_j = 90°$, scaled by $B(\theta_j)$ and the Euclidean volume:

$$R(\theta_j) = \frac{4\pi}{3} D_h^3 R_{Low} B(\theta_j). \qquad (8)$$

4 RESULTS

We have focused on the sensitivity of *Swift* for detecting SGRBs, and highlight several important issues. The complex triggering algorithm of the BAT is biasing detection against SGRBs, and this should be considered when attempting to estimate an intrinsic rate density of SGRBs. The rate estimates using V_{max} are sensitive to the flux limit of the detector, but are mostly invariant to the bolometric and k-correction because these effects cancel out. We also note that SFR evolution may increase the calculated SGRB rate density by ~ 2 in the small-z regime.

Table 2. The beaming-corrected SGRB rate densities with Poisson uncertainties using the observed constraints on θ_j, and scaled by the probability $P_{i(T_{90};P_L)}$, except GRB 100816A, which uses just the T_{90}. Lower rate estimates assume isotropic emission, and upper rates use the observed beaming angle constraints shown in Table 1, or the smallest observed beaming angle in the sample*, $\theta_j \approx 7°$. We calculate the SGRB-EE rate density separately, noting that T_{90} is generally much larger than 2 s, as shown in Table 1.

SGRB	$P_{i(T_{90};\ P_L)}$	Lower rate (Gpc^{-3} yr^{-1})	Upper rate (Gpc^{-3} yr^{-1})
101219A	0.79	0.039	5.3*
100117A	0.89	0.039	5.2*
090510	0.89	0.02	2.7*
080905A^a	0.72	4.9	660*
070724A	0.84	0.77	140
061217	0.89	0.2	27*
051221A	0.72	0.026	3.5
050509B	0.79	2	270*
Total rate		8^{+5}_{-3}	1100^{+700}_{-470}
SGRB-EE			
071227		0.038	0.97
070714B		0.0036	0.66
061210		0.0034	0.16
061006		0.0088	1.6
060614		0.073	3.3
050724		0.03	0.32
Total rate		$0.16^{+0.15}_{-0.088}$	$7.1^{+6.9}_{-4}$

^{a} Because of the importance of GRB 080905 for the rate density and its uncertainty (see Table 1 for caveats), we also calculate total rates excluding this burst, i.e. $(3^{+2}_{-1} - 500^{+340}_{-220})$ Gpc^{-3} yr^{-1}.

With the above caveats, Table 2 shows the rate densities of SGRB and SGR-EE using equation (7) applied to each burst, with the observed constraints on θ_j. The total lower and upper rate densities for SGRBs are 8^{+5}_{-3} (assuming isotropic emission) and 1100^{+700}_{-470} Gpc^{-3} yr^{-1} (assuming beaming – see Table 2) respectively, where the errors are the 95 per cent Poisson statistics (Gehrels 1986). The SGRB rate density is dominated by GRB 080905A, which was relatively faint and nearby, with a $z_{max} \approx 0.3$. Because of the uncertainty in the redshift of this burst, we also calculate a rate density excluding GRB 080905A, and find total and upper rate densities of $(3^{+2}_{-1} - 500^{+340}_{-220})$ Gpc^{-3} yr^{-1}. To test the robustness of the total rate density given that only a few SGRBs contribute significantly to the sum, we used 'jackknife' on the summed SGRB rates in Table 2. The standard error was found to be ±240 Gpc^{-3} yr^{-1}, which is less than the Poisson counting error and the beaming angle uncertainty.

For SGRB-EEs, we find a corresponding rate density of $0.16^{+0.15}_{-0.088}$ and $7.1^{+6.9}_{-4}$ Gpc^{-3} yr^{-1}, respectively. We note that these rates assume $n = 1$ cm^{-3}. If a smaller circumburst density similar to the SGRB is used, the rates will increase by a factor of about 2. It is interesting that the SGRB-EE rate density from this work is similar to the expected BH-NS merger rates from population synthesis models (Ab10).

Assuming that a significant fraction of binary NS mergers produce SGRBs, it is interesting to compare these rate estimates to the NS-NS merger rate density estimated from other work. Our lower rate density, which assumes isotropic emission, is compara-
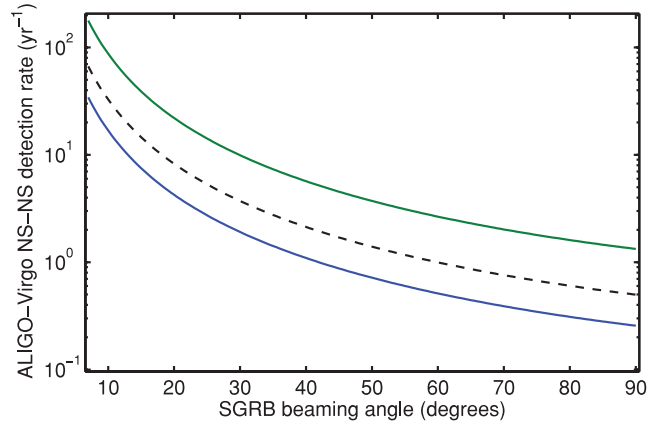

Figure 1. The lower curve plots equation (8), the detection rate of binary NS mergers by a single aLIGO interferometer ($D_h = 197$ Mpc) as a function of the SGRB beaming angle, using $R_{Low} = 8$ Gpc^{-3} yr^{-1} (see Table 2). The upper curve assumes a coincidence search with aLIGO and Virgo interferometers with $D_h = 341$ Mpc. Both horizon distances used to calculate detection rates are angle averaged over all binary orientations. The dashed curve is the same as the upper curve but using the upper rate excluding GRB 080905 (see Table 1 for caveats).

ble to the isotropic emission estimates of Guetta & Piran (2006), i.e. 8–30 Gpc^{-3} yr^{-1}. Our upper limit is comparable to estimates of beamed emission, 240–1500 Gpc^{-3} yr^{-1}. Compared to Ab10, our limits of 7–1200 Gpc^{-3} yr^{-1} are similar to their low-realistic rate densities 10–1000 Gpc^{-3} yr^{-1}.

Finally, we estimate a plausible detection rate by aLIGO/Virgo using the SGRB rate density limits and equation (8). The corresponding lower and upper detection rates using the SGRB rates from Table 2 are 0.2–40 yr^{-1} for a single interferometer with $D_h = 197$ Mpc. Ab10 give a detection rate for aLIGO of 0.4, 40 and 400 yr^{-1} for low, realistic and high detection rates, respectively. In our study, an optimal coincidence search at aLIGO/Virgo sensitivities, with $D_h = 341$ Mpc, the detection rate increases to 1–180 yr^{-1}.

Fig. 1 plots the detection rate for a single aLIGO interferometer ($D_h = 197$ Mpc) and an optimal coincidence search with aLIGO/Virgo ($D_h = 341$ Mpc), as a function of the SGRB beaming angle using equation (8). We use the SGRB rate density 8 Gpc^{-3} yr^{-1} (see Table 2) that assumes isotropic emission.

Our detection rate is similar to the lower and realistic rates based on population synthesis simulations using Galactic pulsar observations. The rates are also compatible with those of Guetta & Piran (2006), who employ a luminosity function and SGRB rate evolution.

5 DISCUSSION

It has been suggested that the observed SGRB population is presently not a useful constraint on rate estimates for compact binary mergers (Ab10). The justification of this argument stems from the fraction (if any) of binary NS mergers that will produce an SGRB. Another issue is that SGRB observations by *Swift* and subsequent follow-up in optical are affected by selection effects and uncertainty in the beaming angles. If SGRB/SGRB-EE have an intrinsic average beaming angle of $\sim50°$, then the jet-break times may not occur until weeks after the burst, when the afterglow is too faint in the optical.

The SGRB rate density depends on the spatial distribution of the sources, but because redshift measurement depends on a bright afterglow, the spatial distribution is biased to the brighter bursts that are nearby (Coward et al. 2008; Coward 2009; Imerito et al. 2009). Hence, for the majority of bursts with a faint afterglow, redshift measurement is more difficult. We attempt to crudely correct for this bias by boosting the calculated rate by the fraction of bursts without measured redshift to those with redshift, assuming that the missing redshifts follow the same distribution as the observed redshifts. This assumption is reasonable (in this work) because the rate density is dominated by those faint bursts in the smallest V_{max}.

Hence, there are two main sources of selection effects and biases. First, there are the satellite detectors, exemplified by the significant difference between BATSE and *Swift* SGRB detection efficiencies. Secondly, there is the problem of obtaining a redshift either from the host galaxy or the afterglow itself (as highlighted above). We have shown that these detection biases should be considered when attempting to use the current (and future) SGRB detections for constraining rate evolution, rate densities and linking SGRBs to binary NS mergers.

The binary NS gravitational-wave detection rate estimates are based on calculating an intrinsic SGRB rate density using *Swift* localized bursts, taking into account dominant selection effects. This approach based on observational data is very different from that based on Galactic binary pulsar observations and modelled population synthesis. In the latter, Ab10 use the observed Galactic binary pulsar population and extrapolate an NS merger rate density out to the aLIGO and Virgo detection horizon. Conversely, our approach avoids this extrapolation because it is essentially an observed rate extending well beyond the average sensitivity distances of the upcoming gravitational-wave searches for compact binaries (about 300 Mpc or $z = 0.07$ for aLIGO and Virgo interferometers) and, moreover, a significant fraction of SGRBs are observed in association with evolved stellar populations.

In conclusion, the upcoming gravitational-wave detection era will be fundamental for resolving the SGRB–binary NS merger connection, since an unequivocal association between SGRBs and binary NS mergers will only be possible via coincident gravitational-wave and electromagnetic observations. Ultimately, a comparison between the SGRB rate density and the gravitational-wave detection rate will help constrain the fraction of binary NS mergers that give rise to SGRBs and the SGRB beaming angle distribution.

ACKNOWLEDGMENTS

REFERENCES

Abadie J. et al. LIGO Scientific Collaboration, 2010, Class. Quantum Grav., 27, 173001 (Ab10)
Ackermann M. et al., 2010, ApJ, 716, 1178
Band D. L., 2003, ApJ, 588, 945
Band D. L., 2006, ApJ, 644, 378
Belczynski K., Taam R. E., Kalogera V., Rasio F. A., Bulik T., 2007, ApJ, 662, 504
Berger E. et al., 2005, Nat, 438, 988
Berger E. et al., 2007, ApJ, 664, 1000
Berger E., Cenko S. B., Fox D. B., Cucchiara A., 2009, ApJ, 704, 877
Bloom J. S. et al., 2007, ApJ, 654, 878
Bromberg O., Nakar E., Piran T., Sari R., 2012a, ApJ, 749, 110
Bromberg O., Nakar E., Piran T., Sari R., 2012b, Proc Sci., SISSA, The Extreme and Variable High Energy Sky, Chia Laguna, p. 031 (arXiv:1112.5949)
Bucciantini N., Metzger B.D., Thompson T. A., Quataert E., 2012, MNRAS, 419, 1537
Caito L. et al., 2010, A&A, 521, A80
Cohen E., Piran T., 1995, ApJ, 444, L25
Coward D. M., 2005, MNRAS, 360, L77
Coward D. M., 2009, MNRAS, 393, L65
Coward D. M., Guetta G., Burman R. R., Imerito A., 2008, MNRAS, 386, 111
Coward D. M. et al., 2011, MNRAS, 415, L26
Della Valle M., 2006, Nat, 444, 1050
Dietz A., 2011, A&A, 529, A97
Eichler D., Livio M., Piran T., Schramm D. N., 1989, Nat, 340, 126
Fong W., Berger E., Fox D. B., 2010, ApJ, 708, 9
Fong W. et al., 2011, ApJ, 730, 26
Fong W. et al., 2012, preprint, arXiv:1204.5475
Gehrels N., 1986, ApJ, 303, 336
Gehrels N. et al., 2004, ApJ, 611, 1005
Gehrels N. et al., 2005, Nat, 437, 851
Gendre B., Corsi A., Piro L., 2006, A&A, 455, 803
Graham J. F. et al., 2009, ApJ, 698, 1620
Gruber D. et al., 2012, in Rau A., Greiner J., eds, Gamma-Ray Bursts 2012. PoS (GRB2012), 36
Gruppe et al., 2006, ApJ, 653, 462
Guetta D., Della Valle M., 2007, ApJ, 657, L73
Guetta D., Piran T., 2006, A&A, 453, 823
Hjorth J. et al., 2003, Nat, 423, 847
Horváth I., Balázs L. G., Bagoly Z., Veres P., 2008, A&A, 489, L1
Imerito A., Coward D. M., Burman R. R., Blair D. G., 2009, MNRAS, 399, L108
Kalogera V. et al., 2006, ApJ, 601, L179
Kopac D. et al., 2012, MNRAS, 424, 2392
Lee W. H., Ramirez-Ruiz E., Granot J., 2005, ApJ, 630, L165
MacFadyen A. I., Woosley S. E., 1999, ApJ, 524, 262
Metzger B. D., Quataert E., Thompson T. A., 2008, MNRAS, 385, 1455
Narayan R., Piran T., Shemi A., 1991, ApJ, 379, L17
Narayan R., Paczynski B., Piran T., 1992, ApJ, 395, L83
Norris J. P., Bonnell J. T., 2006, ApJ, 643, 266
Norris J. P., Gehrels N., Scargle J. D., 2011, ApJ, 735, 23
Paczynski B., 1998, ApJ, 494, L45
Page K. L. et al., 2006, ApJ, 637, L13
Perley D. A. et al., 2009, ApJ, 696, 1871
Piran T., 1992, ApJ, 389, L45
Reddy N. A., Steidel C. C., 2009, ApJ, 692, 778
Rowlinson A. et al., 2010, MNRAS, 408, 383
Sari R., Piran T., Halpern J. P., 1999, ApJ, 519, L17
Soderberg A. M. et al., 2006, ApJ, 650, 261
Stanek S. K. et al., 2003, ApJ, 591, L17
Troja E., King A. R., O'Brien P. T., Lyons N., Cusumano G., 2008, MNRAS, 385, L10
Veres P., Bagoly Z., Horváth I., Mészáros A., Balázs L. G., 2010, ApJ, 725, 1955
Woosley S. E., 1993, ApJ, 405, 273
Yonetoku D., Murakami T., Nakamura T., Yamazaki R., Inoue A. K., Ioka K., 2004, ApJ, 609, 935
Zhang B. et al., 2007, ApJ, 655, L25
Zheng Z., Ramirez-Ruiz E., 2007, ApJ, 665, 1220

This paper has been typeset from a TeX/LaTeX file prepared by the author.